

ACCEPTED MANUSCRIPT • OPEN ACCESS

## Flexible tag design for semi-continuous wireless data acquisition from marine animals

To cite this article before publication: Muhammad Akram Karimi *et al* 2019 *Flex. Print. Electron.* in press <https://doi.org/10.1088/2058-8585/ab423f>

### Manuscript version: Accepted Manuscript

Accepted Manuscript is “the version of the article accepted for publication including all changes made as a result of the peer review process, and which may also include the addition to the article by IOP Publishing of a header, an article ID, a cover sheet and/or an ‘Accepted Manuscript’ watermark, but excluding any other editing, typesetting or other changes made by IOP Publishing and/or its licensors”

This Accepted Manuscript is © 2019 IOP Publishing Ltd.

As the Version of Record of this article is going to be / has been published on a gold open access basis under a CC BY 3.0 licence, this Accepted Manuscript is available for reuse under a CC BY 3.0 licence immediately.

Everyone is permitted to use all or part of the original content in this article, provided that they adhere to all the terms of the licence <https://creativecommons.org/licenses/by/3.0>

Although reasonable endeavours have been taken to obtain all necessary permissions from third parties to include their copyrighted content within this article, their full citation and copyright line may not be present in this Accepted Manuscript version. Before using any content from this article, please refer to the Version of Record on IOPscience once published for full citation and copyright details, as permissions may be required. All third party content is fully copyright protected and is not published on a gold open access basis under a CC BY licence, unless that is specifically stated in the figure caption in the Version of Record.

View the [article online](#) for updates and enhancements.

# Flexible tag design for semi-continuous wireless data acquisition from marine animals

Muhammad Akram Karimi<sup>1</sup>, Qingle Zhang<sup>2</sup>, Yen Hung Kuo<sup>1</sup>, Sohail Faizan Shaikh<sup>1</sup>, Altynay Kaidarova<sup>1</sup>, Nathan Gerald<sup>3</sup>, Muhammad Mustafa Hussain<sup>1</sup>, Jurgen Kosel<sup>1</sup>, Carlos M. Duarte<sup>3</sup>, Atif Shamim<sup>1</sup>

<sup>1</sup>Electrical Engineering, King Abdullah University of Science and Technology, Thuwal, Saudi Arabia

<sup>2</sup>Electronic Engineering, City University of Hong Kong, Kowloon Tong, Hong Kong

<sup>3</sup>Red Sea Research Centre-King Abdullah University of Science and Technology, Thuwal, Saudi Arabia

E-mail: muhammadakram.karimi@kaust.edu.sa

Received January 20, 2019

Accepted for publication xxxxxx

Published xxxxxx

## Abstract

Acquisition of sensor data from tagged marine animals has always been a challenge. Presently, there are two extreme mechanisms to acquire marine data. For continuous data acquisition, hundreds of kilometers of optical fiber links are used which in addition to being expensive are impractical in certain circumstances. On the other extreme, data is retrieved in an offline and invasive manner after removing the sensor tag from the skin of the animal. This paper presents a semi-continuous method of acquiring marine data without requiring tags to be removed from the sea animal. Marine data is temporarily stored in the on board memory of the tag and is then automatically synced to floating receivers as soon as the animal rises to the water surface. To ensure effective wireless communication in an unpredictable environment, a quasi-isotropic antenna has been designed that works equally well irrespective of the orientation of the tagged animal. In contrast to existing rigid wireless devices, the tag presented in this work is flexible and thus convenient for mounting on marine animals. The tag has been initially tested in air as a standalone unit with a communication range of 120 m. During tests in water, with the tag mounted on the skin of a crab, a range of 12 m has been observed. In a system-level test, the muscle activity of a small giant clam (*Tridacna maxima*) has been recorded in real time via the non-invasive wireless tag.

Keywords: Flexible sensors, Wireless communication, Marine animals

## 1. Introduction

Human activities such as deep-sea oil exploration have profoundly affected sea life. Such activities have caused the creation of new habitats for sea animals as a result of changes in physical and biological parameters of the sea. These activities have threatened the survival of rare species. In order to reduce the impact of human activities on the sea, efforts are being made to study these changes by sensing environmental parameters (such as water density, temperature, pressure, oxygen level and pollutants) of the sea as well as the activity level of different sea animals [1] [2] [3] [4]. For example, Beer studied the diversity and abundance of sharks in marine protected areas (MPA) using baited remote underwater video recording [5]. Researchers have also used

permanently installed radio frequency identification (RFID) reader networks to track the movement of seabirds (penguins) when they come out of sea [6]. However, transferring the marine animal data from within the sea up to the surface has always presented difficulties.

The water surface has been a challenging barrier for the communication of marine (underwater) data to air. Acoustic and sonar signals used for underwater communication reflect strongly off of the surface of the sea and cannot propagate across it. In order to enable continuous data communication between seawater and air, researchers have proposed hybrid mechanisms combining acoustic waves with radio frequency waves [7]. However, acoustic waves consume significant amount of energy, increasing the size of

the battery required for long underwater operational life of the tag.

In addition to such hybrid approaches, scientists have used a Real-Time Seafloor Observatory method for continuous data recording which is a fully integrated system consisting of multidisciplinary sensors and other auxiliary devices [8] [9]. The operating rule is that sensors data sampling is performed underwater and transmitted via long optical fiber link or advanced pop-up buoys. This monitoring system is bulky and expensive, prohibiting its use in offshore areas and large-scale monitoring.

Animal-borne video system and data recorder has also been used by researchers to study, for example, the hunting behavior of marine mammals [10].

Scientists have also retrieved marine data in an offline manner by detaching the sensor tag from the skin of the marine animal [11]. The detaching process is not only invasive but is also impractical most of the time. Moreover, weeks or even months may elapse before data can be retrieved. For example, Fletcher was able to retrieve the sound, depth and diving pattern data of seals after 6 days when they returned to rookery [12].

In this paper, we propose a semi-continuous wireless communication data acquisition system to retrieve the sensor data from sea animals, as shown in Figure 1. The proposed system comprises two major components: 1) a flexible wireless tag with built-in flash memory to be placed on the sea animals, and 2) RF receivers floating on the water surface (typically in a marine protected area). The built-in flash memory of the transceiver saves sensor data when the tagged

sea animal is deep under water. As soon as the sea animal comes to the surface, the wireless tag automatically syncs the stored data to the floating RF receiver, allowing non-invasive data readout. This way the data can be transferred in a semi-continuous fashion, i.e., with the emergence of the marine animal to the surface. The proposed system is suitable for most marine animals that rise to the sea surface regularly, such as sharks and dolphins.

The focus of this paper is on the first component of the system, the flexible wireless tag for marine animals. The key element of the wireless tag is the antenna which has been designed so that it radiates in all directions. The tag is flexible for convenient mounting on the marine animal and works equally well in flat as well as flexed conditions. Communication performance of the tag has been tested in air as well as in water with a communication range of 120 m and 12 m, respectively.

The proposed tag provides a common platform for integration and wireless readout of various sensors [11]. The feasibility of the proposed communication platform has been validated by integrating it with a magnetic sensor. This could be helpful for many applications involving monitoring of marine animals. In this work, we have utilized this magnetic wireless sensor tag for detecting muscle movements of a clam floating in water.

## 2. Tag Design

An important consideration for the tag design is to keep it thin, lightweight, and flexible. That is why the tag has been implemented on a flexible medium with a special fabrication

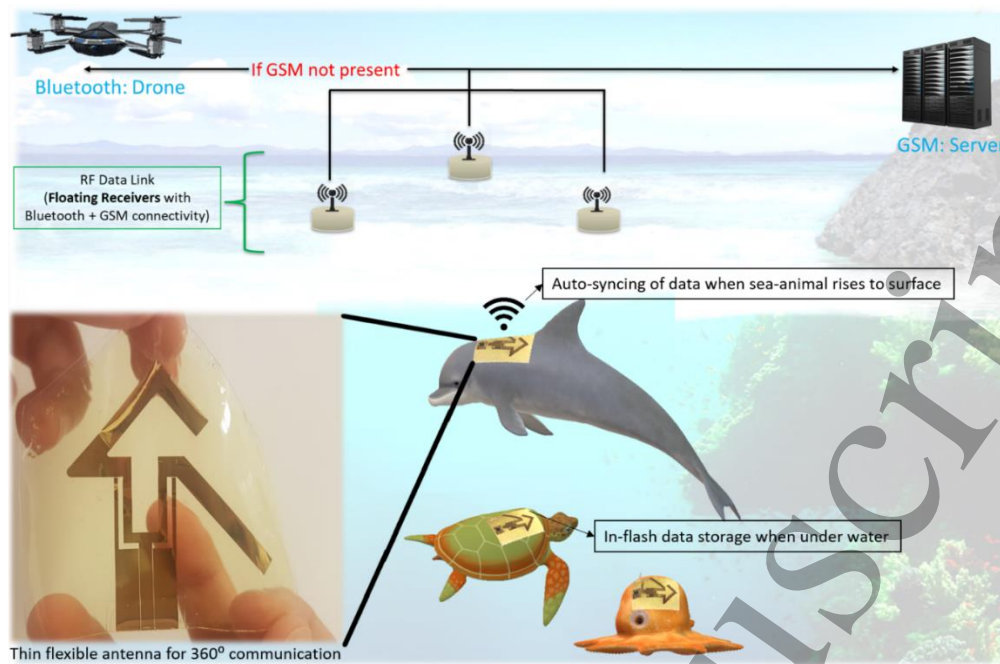


Figure 1. System illustration of a hybrid semi-continuous wireless data acquisition system for marine animals.

technique (discussed later). The antenna, which is typically the largest part of a wireless system, has been designed with two considerations: 1) it is planar and works well in flat as well as flexed conditions, 2) it radiates almost equally in all directions (near-isotropic fashion) to enable orientation-insensitive communication. Another important consideration is to design the system with as low power consumption as possible so that it can operate underwater and above the surface for long periods. The wireless system is thus designed around the Bluetooth Low Energy (BLE) protocol due to its low power consumption.

The proposed system architecture requires the tag to store the sensor data in onboard flash memory. A BLE transceiver with sufficient internal storage has been chosen so that ample amounts of sensor data can be stored in between the syncing cycles (cycles where tag emerges above the surface, synchronizes with the nearby floating receiver, and offloads the data from the memory to the receiver). In addition, the BLE transceiver has the appropriate interfaces required to liaison with a wide variety of digital or analog sensors.

The details of the system are described in the following sections.

### 2.1. Wireless Sensing Tag

To demonstrate a practical marine sensing application, the tag has been integrated with a CMOS magnetic sensor that can sense varying magnetic fields. Many moving parts of a marine animal can be monitored by placing soft, flexible magnets

(discussed later) on those parts and by mounting the magnetic sensor-enabled tag on marine animal body near these magnets. The system is powered using a coin cell battery (225 mAh capacity) and owing to low power consumption of the system, it can run for months without requiring a recharge. A block diagram of the data acquisition system along with the sensor is shown in Figure 2. As depicted in the figure, the system consists of three main parts (shown in blue) and are detailed in the following sub-sections.

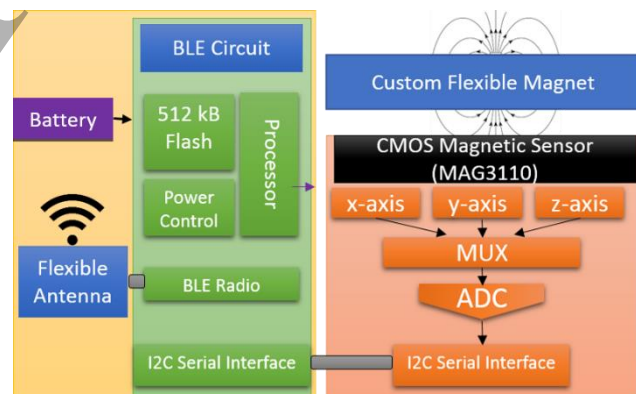


Figure 2. Block diagram of a miniaturized wireless data acquisition system using flexible antenna and flexible magnet.

### 2.2. Antenna Design

One of the major challenges in designing such a wireless system is to ensure robust wireless communication irrespective of the orientation of the flexible tag, because the position and orientation of the marine animals are

unpredictable. Many omnidirectional antennas exist to allow radiation in the shape of a donut, but these do not cover a 360° sphere without radiation nulls. To realize the system concept illustrated in Figure 1, we have designed a near-isotropic antenna that covers the full 360° sphere to ensure reliable data communication irrespective of the orientation of the animal. This has been achieved while keeping the antenna thin, planar, and flexible.

In this new design for a planar flexible antenna with near-isotropic radiation (shown in the bottom left corner of Fig. 1), a Wilkinson divider has been employed to excite the two orthogonal monopoles with equal amplitudes. A 90° phase delay has been maintained between these signals, which is the key to generating near-isotropic radiation. The phase difference has been obtained by adjusting the lengths of the monopoles.

The antenna design has been shown in Fig 3(a) while the design details have been mentioned in the supplementary section. A waterproofing layer entirely covers the circuitry and antenna to ensure proper operation under water.

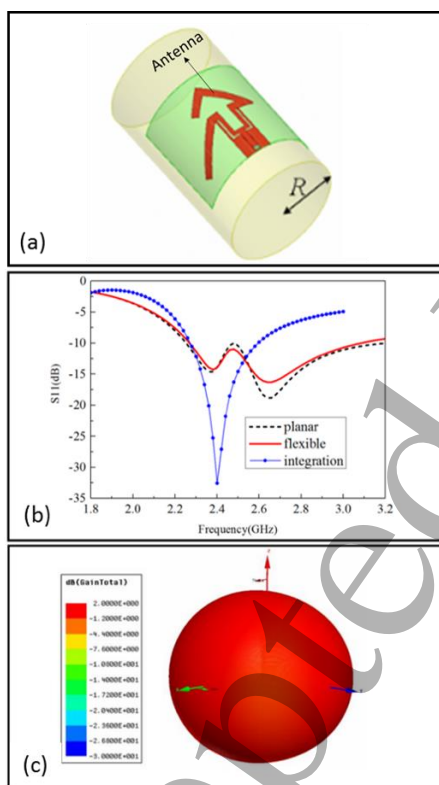


Figure 3. Simulated performance of the antenna. (a) Simulation design of antenna mounted on a curved surface (b) S11 plot showing the impedance matching in normal, flexed and chip-integration states. (c) Radiation pattern at 2.45 GHz.

The antenna has been designed and simulated in Ansys HFSS software. The two most important design parameters of the antenna, impedance matching and radiation performance,

have been optimized, as shown in Figure 3. The antenna reflection coefficient (S11), as shown in Figure 3(a), has a magnitude less than -10 dB in the frequency range from 2.3 to 2.5 GHz. This means that the antenna has good impedance matching in the BLE frequency band. As a result, more than 90% of the RF power can be transferred to the antenna from the driving circuits. It should be noted that antenna impedance stays matched (below -10 dB) even when the antenna is flexed (shown by red curve) or integrated with the Bluetooth transceiver chip (shown by blue curve). Additionally, Figure 3(b) shows that the antenna radiates RF power equally well in all directions (almost uniformly in the 360° sphere), which was one of the major goals for this antenna design. Design details of the antenna are included in the methods section.

### 2.3. CMOS Magnetic Sensor with Soft Magnets

As mentioned above, a CMOS magnetic sensor has been integrated with the wireless tag to demonstrate a practical marine animal monitoring application. Soft flexible magnets are mounted on the moving parts of the marine animal (such as a turtle neck or fish fin). Movement of these parts then creates magnetic field variations on 3D axes which can be detected by the CMOS magnetic sensor (MAG3110). The sensed data can eventually be transferred through the integrated BLE transceiver (Nordic nRF52832). The BLE transceiver reads the sensor data every 100 msec and saves it in internal flash storage (512 kB). This data is offloaded to the floating receivers whenever the tag establishes a wireless connection with them.

For this application, minimally intrusive magnets designed by Kaidarova et al. have been utilized [13]. These NdFeB/polydimethylsiloxane (PDMS) based magnets are chosen for their light weight and flexible nature, which is very convenient for attaching them to marine animal skin. Kaidarova et. al. showed almost three times weight reduction as compared to commercial permanent magnets. Moreover, these flexible magnets coated with 2 μm thick Parylene C polymer have demonstrated excellent corrosion resistance, flexibility, and enhanced biocompatibility. These magnets showed almost no effect on their remanence magnetization even after being submerged in seawater for 70 days.

Many applications can be realized by detection of the varying magnetic fields of these flexible magnets. Examples of data that can be collected this way include movement of fins, gills, turtle legs, clam shells and dolphin body curvature. In this paper, we demonstrate real-time monitoring of the shell movement of a small giant clam by attaching the flexible magnet to one of its shells.

## 3. Circuit Design

A BLE transceiver is integrated with the flexible 2.45 GHz antenna. The flexible antenna has an input impedance of  $50 \Omega$ , whereas the output impedance of the radio front end of the BLE chip is  $53-j66$  and thus not matched to the antenna impedance. A shunt capacitance ( $0.8 \text{ pF}$ ) and a series inductance ( $3.9 \text{ nH}$ ) are used to match the chip impedance to  $50 \Omega$  to ensure minimum signal loss due to impedance mismatch, thus maximizing the radiated power.

The BLE chip has been interfaced with the CMOS magnetic sensor, which is basically a 3-axis magnetometer. An I2C serial communication protocol has been utilized for this interface. The BLE chip starts its operation by configuring some of the internal registers of the CMOS magnetometer to set its measurement range, data frequency, and resolution. In our application, the magnetometer has been configured to output 3-axis magnetic strength at an update rate of 10 Hz. This update rate can easily capture the dynamic movements of most marine animals. The magnetic field data is saved in the built-in flash memory as long as the tag is not connected to a receiver. In the meantime, the chip continues to advertise itself with a 128-bit unique identifier. Meanwhile, the floating Bluetooth receiver keeps scanning for this ID and establishes a connection with the transmitter tag as soon as it receives an

advertisement packet with the ID of interest. At this stage of the project, we have used a smartphone in place of the floating receiver, as we used a smartphone application to visualize the recorded data. However, the floating receivers will replace the smartphones for the final deployment of the system in the marine environment.

## 4. Fabrication and System Integration

### 4.1. Fabrication and Packaging

The two main approaches to making flexible electronics are using conductive polymers themselves as active materials or using existing active materials on flexible polymeric platforms. Conventionally, polymeric materials have been the first choice due to their inherent flexibility and mechanical properties. However, for high performance electronic applications, state-of-the-art mature technologies are superior, and the fabricated devices can be flexed and integrated on the polymeric substrates [14] [15] [16] [17]. For our application, we chose polyimide (PI) and polydimethylsiloxane (PDMS) as polymeric materials to provide flexibility in the design of the metallic antenna.

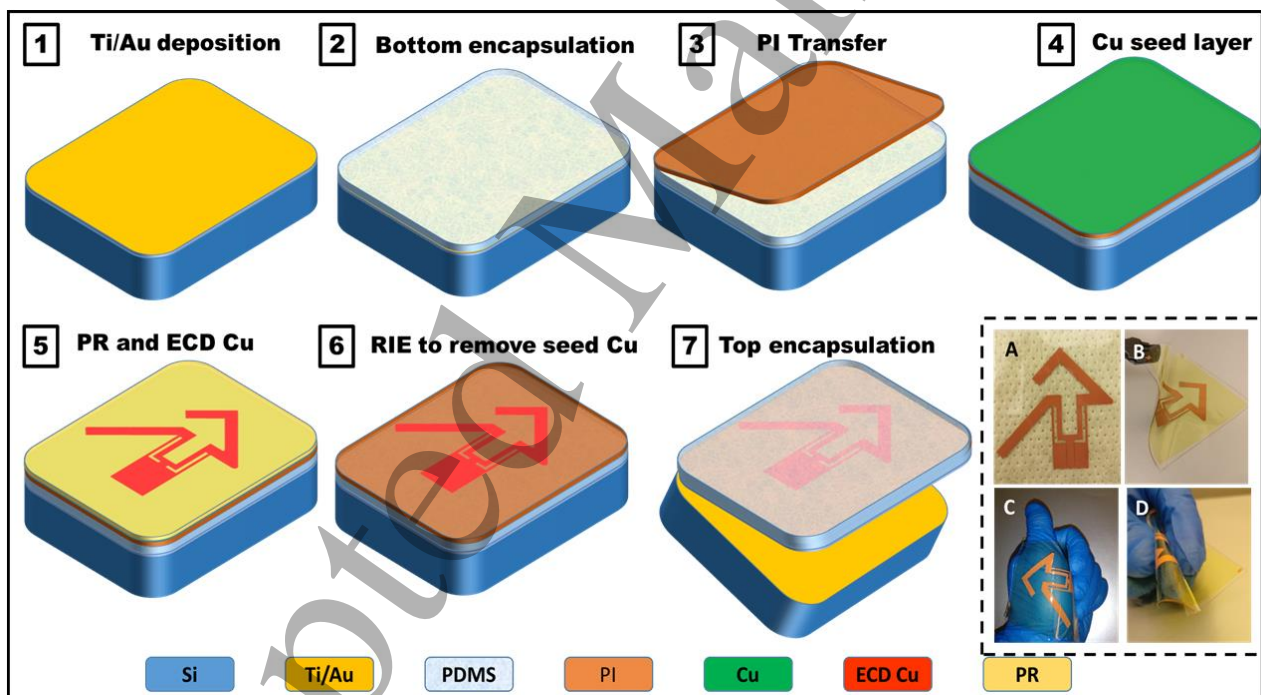


Figure 4. 3D schematic process flow for the fabrication of marine antenna. Inset shows (a) fabricated semi-transparent antenna after peeling off from the wafer substrate. The flexibility of the packaging of the antenna is demonstrated by showing it (b) bending during the peeling process, (c) bent around the thumb, and (d) squeezed between the fingers with bending radius of  $\sim 3 \text{ mm}$ . Scale bars are  $2 \text{ cm}$ .

The fabrication process flow is shown in Figure 4. Gold (Au), as a noble metal, offers high resistance to corrosion implying longer survival in the harsh saline marine environment. However, it is an expensive material and not suitable for a

low-cost application with an antenna that requires a thick metal ( $\sim 5 \text{ um}$ ). Hence, we use a very low-cost metal, copper (Cu), which can be readily deposited to the desired thickness using electrochemical deposition. We deposit Cu film on a 10

$\mu\text{m}$  PI substrate that is non-stretchable but provides mechanical strength without compromising the flexibility of the deposited metal (depicted in Figure 4 b-d). PI was chosen because when metal film is deposited directly on top of other soft polymeric materials, such as PDMS or Ecoflex, it can develop cracks when subjected to physical deformations. One drawback of Cu is its low resistance to corrosion in a saline environment. Therefore, to make the antenna robust in a marine environment without compromising flexibility, we used a soft polymeric packaging strategy (Figure 4). We chose PDMS as a conformal soft packaging material over its counterpart, Ecoflex. PDMS does not undergo decomposition on heat or halogenation, unlike Ecoflex [11] [18] [19] [20]. It is biodegradable, non-toxic, non-irritating to skin, biocompatible, and hydrophobic in nature. It is better suited for integration than Ecoflex because of its compatibility with other process technologies. However, the low surface energy of PDMS due to its hydrophobicity makes it prone to particulate adhesion in aqueous environment [21] [22].

#### 4.2. System Integration

System performance was evaluated in two steps. At first, the flexible antenna was interfaced with the radio front

end of the BLE transceiver on the same flexible substrate using the same fabrication procedure as adapted for the antenna. The custom layout of the transceiver is shown in supplementary Figure S2(a). The fabricated flexible tag, including the antenna interfaced with the transceiver, is shown in Figure 5(a). The antenna performance in this mode will be detailed in the next section.

After validating the antenna performance with the transceiver, the CMOS magnetometer was also integrated via the I2C serial interface. The custom-designed PCB layout for this version is shown in Figure S2(b). The PCB was interfaced with the flexible antenna using bonding wires, and the system was tested by monitoring the activity of a small giant clam (discussed later).

### 5. Results and Discussion

System tests were carried out after confirmation of the radiation and impedance matching performance of the antenna, as these are the key elements needed to ensure efficient communication between the tag and the wireless receiver. Details of these tests are presented in the following sub sections.

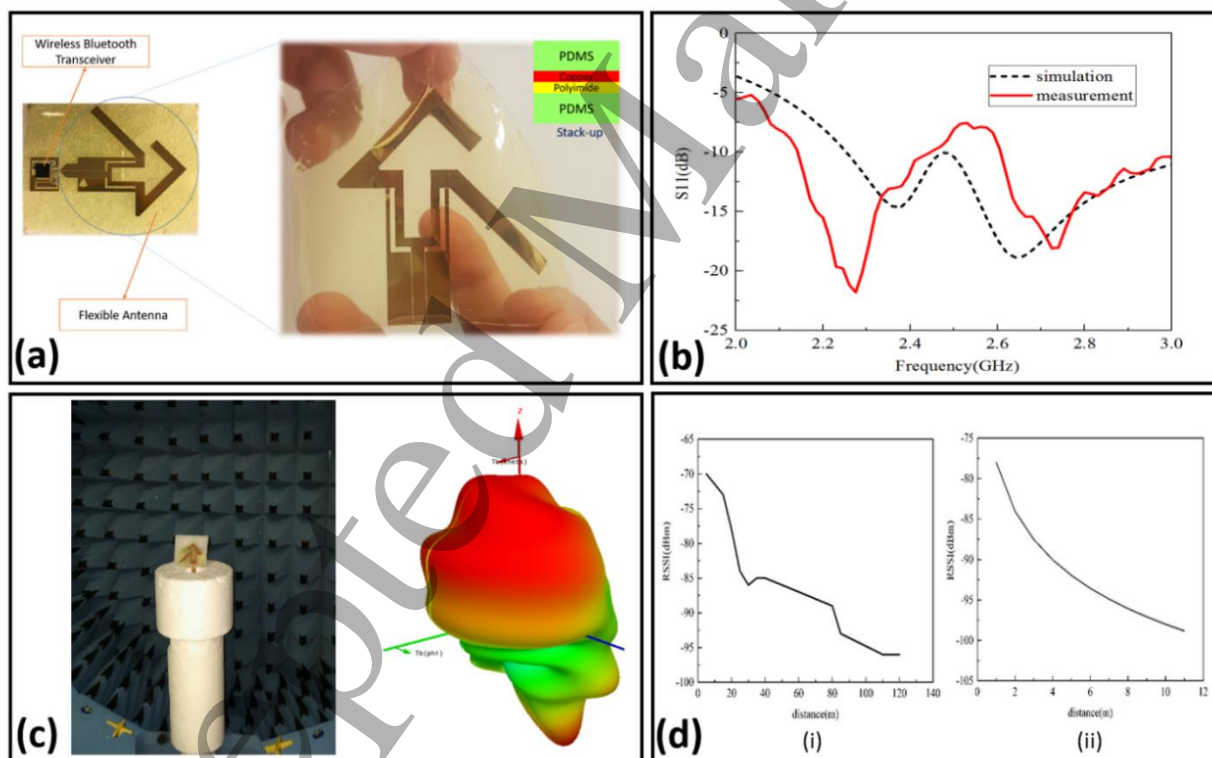


Figure 5. (a) Fabricated flexible tag with near-isotropic antenna integrated with Bluetooth transceiver. (b) Comparison of simulated and measured impedance matching of the antenna; both show good matching (below 10 dB) around Bluetooth operational frequency, i.e. 2.4 GHz. (c) Fabricated antenna placed inside an anechoic chamber to validate its radiation performance (shown alongside). The antenna radiates in all directions (360°) with no NULL. (d) Communication distance of the Bluetooth transceiver in air is around 120 m, while in water (mounted on crab) it is around 8m due to higher dielectric loss of water.

### 5.1. Standalone Antenna Performance

The standalone antenna (shown in the inset of Figure 5(a)) was tested using a SMA connector. The input impedance was measured using a vector network analyzer (VNA) after a careful calibration process. The measured results, shown in Figure 5(b), confirm that the antenna is well matched ( $S_{11}$  below -10 dB) between 2.13 GHz and 3.0 GHz. This result is in good agreement with the simulated result. As intended, this covers the frequency band of BLE (2.45 GHz), and thus the antenna design is capable of efficient radiation in this frequency range due to minimal mismatch loss.

The second step was to test the radiation performance in an anechoic chamber. To conduct this test, the antenna was supported by a piece of foam in order to mount it in the anechoic chamber (antenna radiation pattern measurement chamber), as shown in Figure 5(c). The radiation pattern of the antenna was measured in the 3D space around it using small probes. The measured results demonstrate good radiation all around with a maximum gain of around 0 dB and a gain deviation of 8.5 dB. This is an acceptable gain deviation, and thus we can conclude that the antenna radiates approximately

equally in all directions (i.e., demonstrates near isotropic radiation pattern). As mentioned earlier, this is critical for the intended application in which orientation of the marine animal is unpredictable.

### 5.2. Antenna Integrated Tag Performance

After confirming the performance of the standalone antenna, it was interfaced with the BLE transceiver to validate the performance of the complete tag. The antenna in this case (active mode) was excited by 4 dBm (2.5 mW) power from the BLE chip.

We have developed a smartphone application to measure the received signal strength indicator (RSSI) of the Bluetooth signal received from the flexible tag. For field tests, the smartphone acted as a receiver while the flexible tag acted as a transmitter. In an outdoor environment, the receiver (smartphone with the app) was moved away in steps from the transmitter tag to test the communication range in air. The measured result in Figure 5(d) indicates that the proposed tag can communicate up to a distance of 120 m in air. The same procedure was repeated for testing in water.



Figure 6. Communication range test using smart phone Bluetooth app while the flexible tag is mounted on a crab skin inside the water. (b) System level test of flexible tag to retrieve CMOS magnetic sensor data to detect the movement of the small giant clam.

The flexible tag was partially immersed in water by a few millimeters and, as expected, the communication range was reduced to 12 m due to signal losses in the water. However, it is still sufficient to communicate with floating receivers on the sea surface.

### 5.3. Antenna Performance on Animal Body

The wireless communication performance of the proposed tag was also tested on the body of a marine animal. As depicted in Figure 6(a), the antenna was attached to the surface of a crab inside a water tank. The crab was chosen for initial testing because of the ease of attaching the tag to its surface. A communication range of 8 m was obtained in this

case. This slightly smaller range is probably due to the effect of the animal body and also the walls of the water tank (in addition to the major losses from water itself). Nonetheless, the tag is designed to operate when the marine animal comes to the surface and in that case, the communication range is sufficient.

### 5.4. Activity Monitoring of Small Giant Clam

After validating the communication capability of the tag, when affixed to an animal's body, we integrated a magnetic sensor with the tag to demonstrate the wireless acquisition of sensor data. The activity level of a small giant clam (shown in Figure 6(b)) was monitored for almost 17



minutes, and the data was acquired via the wireless tag. The small giant clam (*Tridacna maxima*) is one of the most sought-after clam species in the aquarium trade. Clam activity level is known to be affected by parameters such as varying oxygen concentration [23] and light intensity [24]. In contrast to using invasive myography techniques to record muscle movement of the clam, we attached permanent magnets to one of the valves (halves) of the clam.

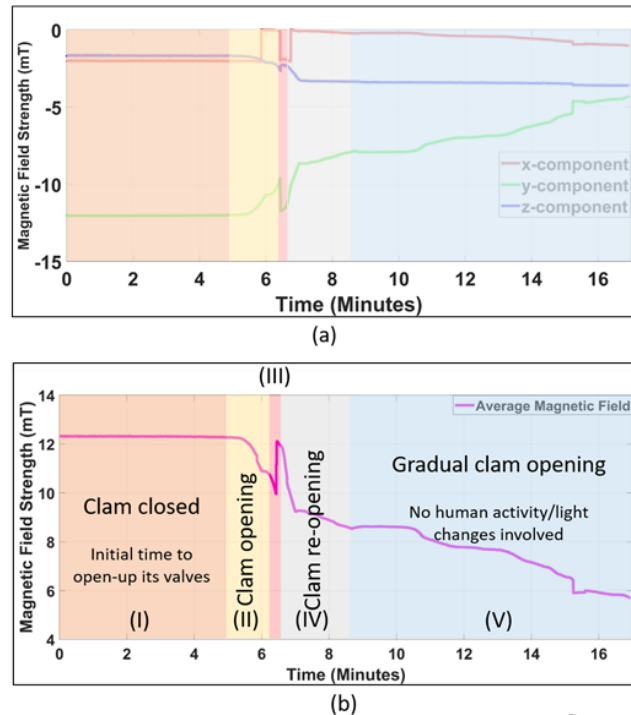


Figure 7. Clam activity data recorded using Bluetooth based mobile phone application. (a) Raw 3-axis magnetic field strength. (b) Averaged magnetic field strength.

The magnetic field emanating from these magnets is detected by the CMOS-based magnetometer<sup>1</sup> which has been integrated with the wireless tag.<sup>2</sup> Any movement of the clam valves results in a varying magnetic field which is measured by the magnetometer in microtesla ( $\mu\text{T}$ ). The BLE transceiver acquires the magnetic field data using the I2C protocol and sends it out wirelessly to the connected Bluetooth device, which can be a smartphone (in a lab environment) or a floating receiver (in a field environment). In this case, we acquired the data using a mobile phone application with an update rate of 10 Hz. It should be noted here that the magnetometer can record the change in magnetic field in 3 axes (i.e. x,y,z), which has been plotted over time in Figure 7(a) while the averaged magnetic field has been plotted in Figure 7(b). From Figure 7(b), it can be clearly seen that the clam passed through different states during the 17 minutes of testing. Thus, various

muscle activities can be easily distinguished from this experiment, as explained below.

The clam was released into the water after attachment of the magnet and the wireless tag to its shell. It can be seen in Figure 7(b) that the clam's valves were closed in the beginning of the test cycle (region I). Most likely, this is because of its self-defense mechanism, as it considered the human who attached the tag to be a predator. In the closed state, the magnet and the tag were in close proximity, which can be seen from the high magnetic field strength recorded in the beginning of Figure 7(b). As the clam was left idle in the aquarium for some time, it started to open up its valves (region II) which moved the magnets away from the wireless tag. This resulted in decreased magnetic field intensity, as can be seen in region II of Figure 7(b). Region III marks the momentary response (closure) of the clam to the change in light intensity. The clam started to reopen itself in region IV, and the movement continued in region V as no further external disturbance was applied to the clam.

For this particular test, the clam was placed near the water surface to ensure continuous wireless data communication. This was done because the clam does not move under water. However, most of the sea animals stay under the water surface and appear on the surface occasionally. For such animals, flash storage and auto-data syncing features have been validated separately. These features will be integrated in the system for future field trials.

## 6. Conclusion

With the emerging concept of the "internet of sea animals," the amount of data gathered from marine life is expected to grow exponentially. This paper has demonstrated a wireless data acquisition system which can be integrated with a wide range of analog and digital sensors and can be mounted onto marine animals in a seamless fashion. To be conformal with the marine animal body, a flexible antenna has been demonstrated which has the capability to communicate effectively in all directions. The sensor data is continuously stored in an integrated flash memory while the animal is under water. The marine tag is then automatically synchronized with the floating receivers on the sea surface, and the stored sensor data is wirelessly transmitted as soon as the animal rises to the surface. The system is designed to allow data acquisition from marine animals without causing any disturbance in their normal activities. The system has been tested to monitor the activities of a small giant clam and useful information regarding the muscle movement has been successfully recorded.

## Acknowledgements

<sup>1</sup> MAG3110 by NXP Semiconductors

<sup>2</sup> Circuit layout of the wireless tag integrated with the magnetometer is shown in Fig.6(b)

Research reported in this publication was supported by the King Abdullah University of Science and Technology (KAUST).

## Supplementary Information

### *Details on Antenna Fabrication*

We designed the antenna for deployment on marine animals in a marine environment, therefore, flexibility and waterproofing were essential requirements of the device. Nassar et al. recently published a detailed fabrication scheme for a compliant lightweight “Marine Skin” tagging system [11] with flexibility and waterproofing for underwater marine environment monitoring. We followed a similar fabrication process with reduced steps and a few modifications, illustrated in the 3D fabrication schematic in Figure 4. We started with a Si carrier wafer with Ti/Au deposited on it. This material was chosen for ease of device removal at the end of the fabrication process. We spun PDMS (thickness = 100  $\mu\text{m}$ ) onto the wafer followed by curing at 75  $^{\circ}\text{C}$  for 75 minutes (Figure 4 step 2). Because metal adheres poorly to PDMS, we used PI 2611 to deposit a metal seed layer. This provides mechanical stability to the whole structure in addition to providing the best adhesion properties. PI was transferred onto the PDMS substrate after being spun to a thickness of  $\sim 10\ \mu\text{m}$  on a second carrier wafer and gradually cured in multiple steps at 90  $^{\circ}\text{C}$ , 150  $^{\circ}\text{C}$  and 350  $^{\circ}\text{C}$  for 90 s, 90 s, and 30 min, respectively. The cured PI was then transferred onto the PDMS wafer followed by seed layer deposition for the copper growth using electrochemical deposition (ECD). 10 nm of Ti and 150 nm of Au metal were sputter deposited as a seed layer on PI using 25 sccm of Ar. ECD of Cu was then performed at an average forward current of 210 mA for 30 minutes ( $\sim 5\ \mu\text{m}$ ), and the growth of Cu was restricted to only the antenna design pattern using 4  $\mu\text{m}$  thick positive photoresist (PR) (Figure 4 step 5). After ECD Cu growth, PR was stripped off using acetone and isopropanol followed by rinsing with deionized (DI) water and drying with  $\text{N}_2$ . The seed layer was removed using physical plasma reactive ion etching (RIE) at 10  $^{\circ}\text{C}$  in the presence of Ar plasma. Final encapsulation of the device to make the antenna waterproof was performed by spinning 150  $\mu\text{m}$  thick PDMS cured at 75  $^{\circ}\text{C}$  for 75 minutes. The fabricated device was then peeled (Figure 4b) from the wafer and characterized for the radiation pattern and S11 parametric measurements.

### *Details on Antenna Design*

Two orthogonal wire monopoles were used to provide equivalent electric responses. The geometry of the proposed antenna, which is fabricated in the PDMS process, is shown in S1(a). A Wilkinson divider was employed to excite the dual orthogonal monopoles (Arm1 and Arm2) with equal magnitude and phase. The divider was realized only on one side of the substrate by 50 ohm coplanar waveguide (CPW) and asymmetrical coplanar strip (ACPS) transmission

lines, which consists of CPW-ACPS tee junction, a pair of ACPS arms, and 2 ACPS outputs except a resistor compared the standard Wilkinson divider.

High Frequency Structure Simulator (HFSS) software was used to simulate the proposed antenna. The resonant frequency mainly depended on the lengths of the dual monopoles  $L_3+L_4$  and  $L_6+L_7$ . By adjusting the lengths of the monopoles [25], the surface currents could have equal magnitude and a 90 $^{\circ}$  phase delay with each other. Figure S1(c) demonstrates the effect of the folded part with length  $L_5$  on the reflection coefficient, while Figure S1(d) shows its effect on radiation performance at 2.4 GHz. It can be observed from Figure S1(c) that impedance matching slightly deteriorated as length  $L_5$  increased. At the same time, parameter  $L_5$  made an important contribution to the quasi-isotropic radiation of the proposed antenna. As plotted in Figure S1(d), when parameter  $L_5$  was 14 mm, the gain deviation at 2.4 GHz was the best at about 4.75 dB, and the reflection coefficient was also acceptable at the operating band. Other antenna parameters also affected the operating frequency and radiation pattern, and the optimized parameters of the proposed antenna are shown in Table 1.

Taking the practical monitoring system of the proposed antenna into account, we also evaluated the performance of the antenna in a flexed state. As illustrated in Figure S1(a), the proposed antenna was tagged on a foam cylinder surface with  $R_1=30\ \text{mm}$  radius. The impedance matching of the flexed antenna was compared with that in the non-flexed state, as depicted in Figure S1(b). It clearly indicates that bending operation of the proposed antenna did not affect the resonant frequency, and the -10 dB bandwidth remained at about 0.76 GHz (2.24 GHz-3.0 GHz).

Figure S1(e) shows the simulated 3D radiation pattern of the proposed antenna at 2.4 GHz in planar state, while Figure S1(f) shows the simulated radiation performance in flexed state. The gain for the planar state was 2.0 dB and the gain deviation was 4.75 dB. For the flexed state, the gain remained 2.2 dB and the deviation became 6.37 dB, which indicates that the proposed antenna maintains good flexible performance with quasi-isotropic radiation. When the proposed antenna was integrated with a balun, the gain was 1.46 dB and the deviation remained at 7.4 dB, and thus the radiation of the proposed antenna remained isotropic. This illustrates that employing an additional balun does not affect the isotropic radiation characteristic of the proposed antenna.

### *Details on Flexible Magnet Fabrication*

First, PDMS was prepared by mixing elastomer and curing agent using a 10:1 weight ratio, and NdFeB microparticles were added by mechanical stirring. The composite was then poured into customized polymethylmethacrylate (PMMA) molds fabricated using a CO2 laser cutter. Aligning NdFeB particles with a magnetic field has been shown to increase remanent magnetization by

~16%, which is attributed to the alignment of an anisotropy axis with the field direction [13]. Therefore, a unidirectional magnetic field of 1.5 T was applied prior to curing the PDMS at 90°C for an hour.

### *Details on PCB Design*

The Bluetooth Low Energy (BLE) communication protocol was chosen due to its low power consumption and compatibility with smartphones. The nRF52832 System on Chip (SoC) from Nordic Semiconductors, which has built in flash storage of 512kB, was chosen for the system. Two custom PCBs were designed using Altium Designer, a PCB design software package. The first of the double layer PCBs had a transceiver integrated with the flexible antenna, the layout of which is shown in S2(a). This 1.96 cm \* 1.74 cm-sized PCB was designed using the nRF52832 with 50  $\Omega$  CPW pads (Ground-Signal-Ground), with which the flexible antenna was connected with the same impedance, i.e., 50  $\Omega$ . The programming header, which also acted as power source for the PCB, was also provided on the PCB to update the firmware whenever needed. A 32 MHz external crystal was used for the main clocking operation of the SoC, while a 32.768 kHz low-frequency crystal was used to save power in

sleep mode. There was an internal Low Dropout (LDO) regulator in the nRF52832 chip to regulate the battery voltage; however, an external LC filter was connected to the PCB to use a DC/DC regulator instead, as it consumes less power than the internal LDO.

The second of the PCBs (shown in S2(b)) had the same programming header, crystal, and DC/DC converter components as the first, with the addition of a CMOS magnetometer, the MAG3110. A few RC components were added for chip enabling purposes and to regulate the power supplied to the chip. The magnetometer interfaced with the nRF52832 over I2C communication lines of SDA (Serial Data) and SCL (Serial Clock). External 10 k $\Omega$  resistors were used on the lines as per the requirements of I2C communication.

### *Details on Smart Phone App*

The connected smart phone application filters out the Bluetooth devices with the specified UUID<sup>3</sup> and can measure their RSSI values. For the experimentation, 4 dBm power was used to advertise the Bluetooth packets from the transmitter PCB.

<sup>3</sup> 128 bit service UUID is 0x 0000 AAAA 1212 EFDE 1523 785F EF13 D123

## References

- [1] S. J. Cooke, S. G. Hinch, M. Wikelski, R. D. Andrews, L. J. Kuchel, T. G. Wolcott, P. J. Butler, "Biotelemetry: a mechanistic approach to ecology," *Trends in Ecology & Evolution*, vol. 19, no. 6, pp. 334-343, 2004.
- [2] B. A. Block, D. P. Costa, G. W. Boehlert, R. E. Kochevar, "Revealing pelagic habitat use: the tagging of Pacific pelagics program," *Oceanologica Acta*, vol. 25, no. 5, pp. 255-266, 2002.
- [3] M. E. Lander, T. Lindstrom, M. Rutishauser, A. Franzheim, M. Holland, "Development and field testing a satellite-linked fluorometer for marine vertebrates," *Animal Biotelemetry*, vol. 3, 2015.
- [4] Y. Ropert-Coudert, R. P. Wilson, "Trends and Perspectives in Animal-Attached Remote Sensing," *Frontiers in Ecology and the Environment*, vol. 3, no. 8, pp. 437-444, 2005.
- [5] A. J. E. Beer, "Diversity and abundance of sharks in no-take and fished sites in the marine protected area network of Raja Ampat, West Papua, Indonesia, using baited remote underwater video (BRUVs)," Royal Roads University, British Columbia, 2015.
- [6] M. Gauthier-Clerc, J. P. Gendner, C. A. Ribic, W.R. Fraser, E. J. Woehler, S. Deschamps, C. Gilly, Y. Le Maho, "Long-term effects of flipper bands on penguins," in *Proc. Roy. Soc. Lond. Biological Sciences*, pp. 423-426, 2004.
- [7] F. Tonolini, F. Adib, "Networking across boundaries: enabling wireless communication through the water-air interface," in *SIGCOMM*, Budapest, 2018.
- [8] K. Kawaguchi, S. Kaneko, T. Nishida, T. Komine, "Construction of the DONET real-time seafloor observatory for earthquakes and tsunami monitoring," in *SEAFLOOR OBSERVATORIES*, Springer, Berlin, Heidelberg, 2015, pp. 211-228.
- [9] P. Favali, R. Person, C. R. Barnes, Y. Kaneda, J. R. Delaney, S. K. Hsu, "Seafloor Observatory Science," in *Proceedings of OceanObs'09*, Venice, 2010.
- [10] R. Davis, L. Fuiman, T. Williams, S. Collier, W. Hagey, S. Kanatous, S. Kohin, M. Horning, "Hunting behavior of a marine mammal beneath the Antarctic fast ice," *Science*, vol. 283, no. 5404, pp. 993-996, 1999.
- [11] J. M. Nassar, S. M. Khan, S. J. Velling, A. Diaz-Gaxiola, S. F. Shaikh, N. R. Gerald, G. A. T. Sevilla, C. M. Duarte, M. M. Hussain, "Compliant lightweight non-invasive standalone "Marine Skin" tagging system," *npj Flexible Electronics 2*, Article number: 13, 2018.
- [12] S. Fletcher, B. J. L. Boeuf, D. P. Costa, P. L. Tyack, S. B. Blackwell, "Onboard acoustic recording from diving northern elephant seals," *The Journal of the Acoustical Society of America*, vol. 100, no. 4, pp. 2531-2539, 1996.

- [13] A. Kaidarova, M. A. Khan, S. Amara, N. R. Geraldi, M. A. Karimi, A. Shamim, R. P. Wilson, C. M. Duarte, J. Kosel, "Tunable, Flexible Composite Magnets for Marine Monitoring Applications," *Advanced Engineering Materials* 1800229, vol. 20, no. 9, 2018.
- [14] A. M. Hussain, M. M. Hussain, "CMOS-Technology-Enabled Flexible and Stretchable Electronics for Internet of Everything Applications," *Advanced Materials*, vol. 28, no. 22, pp. 4219-4249, 2015.
- [15] A. M. Hussain, S. F. Shaikh, M. M. Hussain, "Design criteria for XeF<sub>2</sub> enabled deterministic transformation of bulk silicon (100) into flexible silicon layer," *AIP Advances* 6, 075010, 2016.
- [16] J. M. Nassara, J. P. Rojas A. M. Hussain, M. M. Hussain, "From stretchable to reconfigurable inorganic electronics," *Extreme Mechanics Letters*, vol. 9, no. 1, pp. 245-268, 2016.
- [17] S. F. Shaikh, M. T. Ghoneim, G. A. T. Sevilla, J. M. Nassar, A. M. Hussain, M. M. Hussain, "Freeform Compliant CMOS Electronic Systems for Internet of Everything Applications," *IEEE Transactions on Electron Devices*, vol. 64, no. 5, pp. 1894 - 1905, 2017.
- [18] N. Hammerschlag, S. J. Cooke, A. J. Gallagher, B. J. Godley, "Considering the fate of electronic tags: interactions with stakeholders and user responsibility when encountering tagged aquatic animals," *Methods in Ecology and Evolution*, vol. 5, no. 11, pp. 1147-1153, 2014.
- [19] V. P. Shastri, "Non-Degradable Biocompatible Polymers in Medicine: Past, Present and Future," *Current Pharmaceutical Biotechnology*, vol. 4, no. 5, pp. 331 - 337, 2003.
- [20] J. E. Mark, *The Polymer Data Handbook*, Oxford University Press, 2009.
- [21] S. Krishnan, C. J. Weinman, C. K. Ober, "Advances in polymers for anti-biofouling surfaces," *Journal of Materials Chemistry*, vol. 18, no. 29, pp. 3405-3413, 2008.
- [22] H. Zhang, M. Chiao, "Anti-fouling Coatings of Poly(dimethylsiloxane) Devices for Biological and Biomedical Applications," *Journal of Medical and Biological Engineering*, vol. 35, no. 2, pp. 143-155, 2015.
- [23] D. G. Badman, "Changes in activity in a freshwater clam in response to oxygen concentration," *Comparative Biochemistry and Physiology Part A: Physiology*, vol. 47, no. 4, pp. 1265-1271, 1974.
- [24] T. R. Dork, "Maxima Clam Reacting to Light," 2017. [Online]. Available: <https://www.youtube.com/watch?v=5Zs5htHo5tM>.
- [25] G. Pan, Y. Li, Z. Zhang, Z. Feng, "Isotropic Radiation From a Compact Planar Antenna Using Two Crossed Dipoles," *IEEE Antennas and Wireless Propagation Letters*, vol. 11, pp. 1338 - 1341, 2012.